

Active Power Control on Wind Turbines: Impact on Mechanical Loads

Bernabé Ibáñez  Fernando A. Inthamoussou  and Hernán De Battista 

Abstract—This work focuses on the evaluation of how Active Power Control (APC) impacts the mechanical loads of a utility-size Wind Turbine (WT). Two APC strategies, each with four levels of power reserve, are considered and compared. The assessment is numerically performed over the 5 MW WT benchmark model. Fatigue analysis is carried out under realistic wind profiles and following IEC 61400-1 standard. Extreme load analysis is performed as well, with extreme wind conditions as defined in the standard, and with a statistical load extrapolation from normal wind conditions. The assessment is repeated with both a Linear Parameter-Varying controller and a gain scheduling Proportional Integral controller comprising 3225 simulations. Interesting results are obtained about how APC affects mechanical loads, and how this impact changes according to the control strategy applied. For instance, for some combination of controller scheme and APC strategy, fatigue loading is reduced with respect to maximum power tracking without increasing extreme loads. These results lead to the conclusion that fatigue load can be improved by unevenly distributing power reserve among wind turbines across the wind farm.

Index Terms—wind turbine, load analysis, active power control, power reserve control, fatigue and extreme loads

I. INTRODUCTION

The proper operation of an interconnected electrical grid relies on the continuous balancing between generation and consumption in order to keep the grid frequency constant. To achieve this, forecasts of electrical demand are performed, and power generation is scheduled accordingly. The instant-to-instant demand fluctuations are automatically compensated by the inertia of rotating machines in traditional power plants. That is, when generation exceeds the demand, the rotating machines accelerate, increasing the grid frequency and storing the energy in excess as kinetic energy. Conversely, when demand exceeds generation, the machines slow down diminishing the grid frequency and supplying kinetic energy to the system. Primary frequency regulation is the next step, it uses the droop curve of some generators to lead frequency to its steady-state value. Automatic generation control comes later, modifying the generated power of the capable power plants in the network in order to restore frequency to nominal. At last, power plants previously appointed to have the capacity to increment their generation come into play. This so-called power reserve control, is usually done manually as response to demand forecast [1].

Nowadays, wind energy holds an important role in the electricity market. For instance, it covered the 15% of the

electricity demand of the European Union in 2021, with a maximum penetration of 44% in Denmark [2]. The installed capacity in Latin America and the Caribbean is growing strongly too, reaching 7% of the total capacity in 2020 [3]. Particularly, wind energy supplied 9,6% of the electricity demand in Argentina in 2021 [4]. This increase in the wind energy penetration has risen some alarms, as it is well known the uncertain, variable and asynchronous nature of wind power plants. Uncertainty in the primary resource was not a serious problem while wind penetration to the grids kept low. However, as penetration has risen, wind farms have been increasingly required by grid operators to produce energy below maximum. The primitive way to derate the wind farm is to turn off some Wind Turbines (WTs). Also, their efficiency can be reduced by pitching overriding maneuvers. In recent years, different Active Power Control (APC) strategies have been proposed.

Since the first ideas presented in [5], APC has become one of the control facilities to be offered by modern wind turbines. APC allows wind farms to satisfy the energy demand by adjusting the power output of WTs instead of turning them off and on individually. This method reduces the grid perturbations introduced by the wind energy, and has a higher capacity of providing ancillary services [1]. APC requires the WTs to operate on an extended locus. As a consequence, the existing control system needs to be adapted to this extended control strategy in order to provide wind farms with APC capabilities.

There is an important trend on this line of research in the literature. For instance, [6] presents an Model Predictive Control (MPC) design of a wind farm APC in order to optimize the reference power tracking. In [7], a coordinated APC with combined pitch and rotor speed control is introduced, aiming at improving the rotational speed regulation. Further, the proposal of utilizing the rotor kinetic energy to regulate its rotational speed and diminish the pitch activity following an APC reference is presented in [8]. A novel strategy for power reserve maximization in a wind farm is presented in [9]. Both the Linear Parameter-Varying (LPV) and the gain scheduling Proportional Integral (PI) controllers with APC features to be evaluated in this work are detailed in [10].

In order to raise the capacity of wind power plants, the size of WTs is continuously increasing. The main drawback of this is that the mechanical efforts WTs have to withstand may become critical. This motivates the growing interest in controlling and reducing both fatigue and ultimate loads of WT components. There are several works in the literature regarding different kinds of load analysis and load reduc-

Bernabé, Fernando and Hernán work at Grupo de Control Aplicado (GCA), Instituto LEICI (UNLP - CONICET), Facultad de Ingeniería, Universidad Nacional de La Plata, C.C.91 (1900) La Plata, Argentina

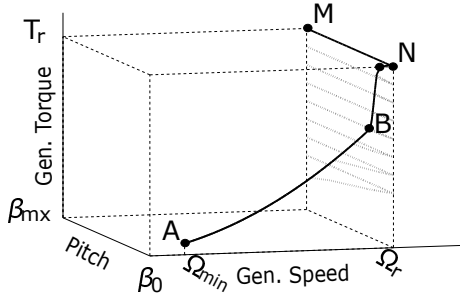


Fig. 1. Torque vs. generator speed for the extended operation.

tion techniques. For instance, [11] presents a multi-variable individual pitch control to mitigate periodic loads above rated. In [12], two controllers based on an active disturbance rejection-based paradigm aiming at getting rid of periodic and non-periodic loads are presented and compared against two baseline controllers. A load mitigation and power tracking controller is presented in [13] for the National Renewable Energy Laboratory (NREL) 5MW benchmark WT, however, it does not cover the full operating range of the WT, leaving out part of below rated wind speeds, which are particularly important when considering tower loads. An exhaustive load analysis comparing a gain scheduling PI and a LPV controller is presented in [14]. In [15], the effects of three power reserve control strategies on structural loading with two levels of power references (90% and 80%) are studied through several simulations and field tests on the 600kW WT CART3, following the IEC standard. The study is performed with a controller designed based on the baseline PI defined in [16], adapting it to the CART3. The study provides relevant results about the power reserve effects on a mid-scale WT, which can be partially extrapolated to larger WTs except for some expected differences that motivate the study of the impact on a larger WT.

In this work, a comprehensive analysis of the effects of different APC strategies over the mechanical loads is provided, following the IEC standard closely [17]. The case-studies considered comprise both fatigue and extreme loads of a utility-size WT facing design scenarios with several levels of power references, and comparing two different controllers: a baseline PI and an LPV. The objective is to evaluate how providing power reserve through APC affects WT loads.

The paper is organized as follows: section 2 presents the system under study and provides an overview of the WT, the controllers and the reserve strategies; section 3 enumerates and summarizes the design load cases and the types of load analysis performed; section 4 presents the results of the simulations and analysis; which are further discussed in section 5; and section 6 contains the conclusions and final thoughts.

The WT model used in the simulations consists on the utility size NREL 5MW benchmark WT. It has a classical configuration of variable pitch (pitch-to-feather) and variable speed. The usual control strategy for a WT with this configuration has two basic control systems: a generator torque controller and a collective pitch controller. Both systems are designed to work separately most of the time.

This strategy follows the curve A-B-N-M in Fig. 1, with different operating regions, i.e.,: In Region 1 (A-B), the generator torque tracks the maximum power curve, with the pitch controller set at its optimum value. In Region 3 (N-M) the pitch controller regulates the rotational speed to maintain it at rated, while the torque controller is fixed at rated as well. Region 2 (B-N) consists on a transition between the main control systems. This Region is critical because both control loops may work simultaneously.

As previously mentioned, it is necessary for the APC to extend the operating regions (Fig. 1). These new extended operating regions result in:

- Region 1e: this region now comprehends the area below the curve A-B, however, the transition could occur before reaching B, since the power reference may be smaller to the one corresponding to point B.
- Region 2e: this region consists now of everything that is under the A-N curve in the torque - rotational speed plane. When the power reference is reached, the operation point moves along the constant power hyperbola until the rated rotational speed.
- Region 3e: contains the area under the N-M line. There, the blades pitch so that the WT can generate the reference power at rated rotational speed.

In this work, four different power references will be considered within each APC strategy: 90%, 80%, 60% and 40% of the available power. They will be contrasted against the baseline strategy: 100% of the available power, i.e., the classical reference (A-B-N-M curve).

The APC is applied for each of them, following two different strategies:

- 1 - Fractional Power Reference (FPR): $P_{Ref} = P_{av} * x$, the power reference (P_{Ref}) is a desired fraction x of the available power (P_{av}) at the wind turbine output, i.e., there is full range power reserve (the available power is limited to the WT rated power).
- 2- Absolute Power Reference (APR): $P_{Ref} = P_r * x$, the power reference is a fraction of the rated power (P_r), i.e., there exists power reserve only in Region 3e.

For a better understanding of the behaviour of FPR and APR strategies, Fig. 2 shows the power references for both of them.

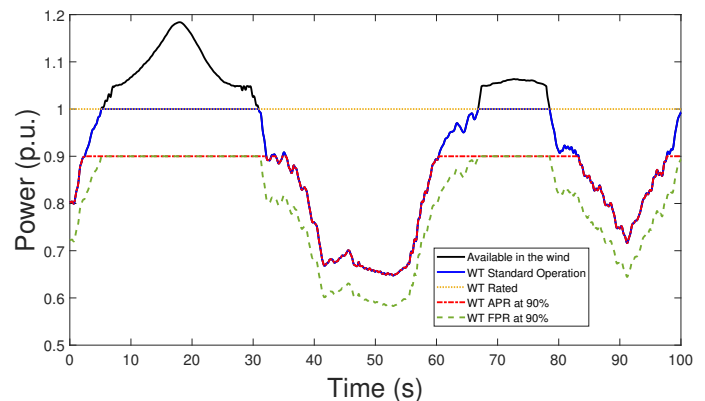


Fig. 2. APC strategies.

It can be seen clearly how APR only provides reserve when the available power is greater than its reference while FPR has full power reserve.

With each of the strategies described, two different controllers will be considered in the simulations and load analysis carried out in this paper: a PI which results from the adaptation of the controller defined in [16], extending its operating region to work with APC as previously described, and an LPV controller (topology shown in Fig. 3). Both controllers are parameterized by the pitch angle of the WT and the normalized power reference. The look-up table block of the controller implements the typical control strategy of the WT, and its output is compared with the power per unit (P_{pu}) to establish the torque reference of the WT. The details of these controllers are explained in [10].

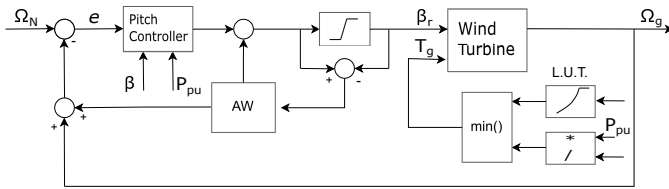


Fig. 3. LPV controller topology

III. LOAD ANALYSIS

The objective of this work is to quantify how APC strategies affect the mechanical loads of the WT. This is done following the IEC standard, considering the Design Load Cases (DLCs) relevant to the control. The standard mentions DLCs that should be considered while designing a WT. These DLCs are categorized in two groups: normal energy production, on the one hand; and energy production with failure, WT start up, turn off and emergency turn off, on the other hand. Besides, within each group, several conditions are listed, for example: Normal Turbulence Mode (NTM) (analyzing extreme and fatigue loads), Extreme Turbulence Mode (ETM), Extreme Coherent gust with Direction change (ECD), Extreme Operating Gust (EOG) with different recurrences, both horizontal and vertical Extreme Wind Shear (EWS) among others, and a turbulent Extreme Wind Model (EWM). These cases are summarized in Table I, where U stands for Ultimate load, and F for fatigue. The mechanical loads considered in this work are illustrated in Fig. 4. Namely, blade root Out of Plane (OOP), In Plane (IP) and Pitching (PT) bending moments, tower base Fore-aft FA and Side-to-side (SS) bending moments and, at last, High Speed Shaft Torque (HSST).

A. Fatigue

The oscillating nature of WT loads results in inflicted damage on WT components and in fatigue damage by accumulation, which could make a component fail. This damage is calculated by separating the loads in individual hysteresis cycles, taking pairs of local minima and maxima (known as Rain-flow counting algorithm [18]). These load cycles can be characterized by their mean value and amplitude. It is assumed that the damage within each load cycle is linearly accumulated according to Palmgren-Miner's Rule [19].

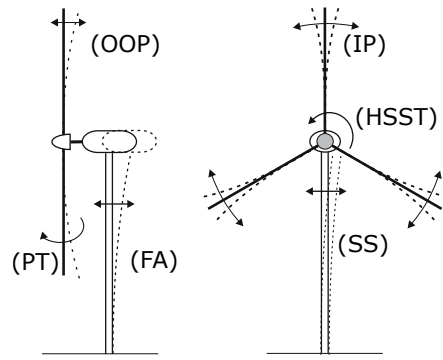


Fig. 4. Mechanical loads

While Miner's rule assumes that structural failure occurs when the cumulative damage parameter equals one ($D = 1$), is important to consider that according to a study by Veers [20], the calculated damage varies widely in WT components, from 0.79 to 1.53. This means that differences between damage and lifetime predictions of the WT components up to a factor of 2 could arise, and further, should be expected.

Aiming at an appropriate estimate of the lifetime damage of WT components, several time series for each mean wind speed are simulated. This is achieved by simulating the WT for a limited amount of time, much shorter than its lifetime, but large enough for obtaining representative conclusions about lifetime loads through statistical extrapolation [17].

These statistical calculations are performed using MLife, a software that works with the time series generated by FAST as inputs. Particularly, for the fatigue analysis along the WT lifetime, the IEC standard [17] establishes that 6 time series of 10 minutes each should be obtained for each mean wind speed. Depending on the selected DLC, MLife extrapolates differently the resulting fatigue of the time series [21].

B. Damage Equivalent Loads

To be able to compare different load spectra, Damage Equivalent Loads (DELs) are defined. A DEL is a constant amplitude and fixed frequency load (with a fixed mean value), that inflicts the same damage as the varying and much more complex load spectra under study.

Aiming to quantify the mechanical loads obtained in a summarized form, the concept of Lifetime Damage Equivalent Load (LDEL) will be used. Similar to DELs but extrapolated to the WT lifetime, the LDEL is a constant amplitude and fixed frequency load that inflicts the same damage as the varying load spectra over the entire lifetime (i.e., 20 years) of a WT exposed to the annual wind distribution of the location [21]. When applying APC, LDELs are obtained assuming that the WT would work its whole lifetime with the same APC strategy. While this is not realistic, it is useful for reaching valid results and comparisons between the strategies and levels of power reference.

C. Extreme Load Analysis

The WT components structural failure may be due to extreme values of mechanical solicitations. These extrema can

appear in extreme wind conditions, although they may also arise due to combinations between unfavorable weather conditions and system failures. The IEC standard considers several extreme values analysis to be performed with the objective of quantifying the worst-case scenario for the extreme extraction in the simulations. The software MExtremes is used for the extraction of these extreme values [22].

D. Statistical Extrapolation of Extremes

As the extreme scenarios simulated may not consider the lower probability events, DLC 1.1 requires the extrapolation of loads whose occurrence probability coincides with a 10-minute interval once in 50 years. To find these values, a mechanical load extreme values extraction is made from the normal turbulence mode. With these, a statistical fitting for each set of data (corresponding to each mean wind speed) is performed. Finally, the cumulative probability function is obtained by means of the previous data fittings, and with it, the 50-year recurrence loads required by the standard are obtained [17], [23].

TABLE I
DESIGN LOAD CASES

Design Situation	DLC	Wind Condition	Type	# Simulations
1. Power Production	1.1	NTM	U	2484
	1.2	NTM	F	
	1.3	ETM	U	414
	1.4	ECD	U	126
	1.5	EWS	U	108
2. Power Production + Occurrence of fault	2.3	EOG	U	72
6. Parked	6.1	EWM 50-y	U	6
	6.3	EWM 1-y	U	12
7. Parked + fault	7.1	EWM 1-y	U	3
Total number of simulations				3225

Details: 1.1 Statistical extrapolation of loads. 2.3 Loss of electrical network. 6.3 Yaw misalignment and 7.1 Blade stuck.

E. Design Load Cases

Table I summarizes the DLCs defined by the IEC that are considered in this paper. With the objective of performing the batch of simulations detailed in the table, several wind files were generated. For the NTM, used in DLCs 1.1 and 1.2, six three-dimensional ten-minutes wind files for each mean wind speed, between 3 and 25 m/s (stepped at 1 m/s) were created with Turbsim using the Kaimal model. It is worthy to mention that this model is accepted by the IEC standard. A Rayleigh annual wind distribution with a mean of 8,5 m/s and a Class B turbulence were considered.

The ETM, used in DLC 1.3, is similar to the NTM, but with a higher turbulence component. For this analysis, one file was generated per each mean wind speed between 3 and 25 m/s (stepped at 1 m/s).

For DLC 1.4, different directions and signs of ECD were considered. Horizontal and vertical EWS for 12 and 24 m/s were used for DLC 1.5. EOG over the cut in, cut out and rated

TABLE II
LPV LDELS VARIATIONS [%].

Lifetime DELs	LPV - FPR				LPV - APR			
	90	80	60	40	90	80	60	40
OOP	4.5	-2.4	-15.5	-21.3	-0.9	-2.9	-10.0	-19.4
IP	-0.5	-1.0	-1.7	-2.3	-0.5	-0.9	-1.6	-2.2
PT	-7.2	-13.7	-25.6	-25.8	-3.3	-7.7	-17.6	-27.0
FA	11.8	5.3	-2.7	-5.7	0.4	0.2	-1.3	-3.9
SS	3.9	2.7	-0.5	-1.8	0.1	0.1	-0.2	-0.8
HSST	40.3	26.4	-4.1	-21.6	-4.0	-10.9	-19.8	-23.0

± 2 m/s wind speeds were generated for DLC 2.3. All these files were obtained using IECWind software [24].

The wind profiles described above were used to perform simulations with both controllers mentioned before: LPV and PI. For each of them, several cases were considered: on the one hand, a baseline strategy (100% of power reference), and on the other hand, two APC strategies: FPR and APR with four power references each: 90%, 80%, 60% and 40%.

For the parked cases, turbulent profiles of EWM of 1-year and 50-year recurrence (with 34 and 42.5 m/s mean wind speed, respectively) were considered. Also, mean yaw misalignment of -20° and 20° were simulated for DLC 6.3. On the other hand, DLC 7.1 was simulated with one blade stuck (two blades with pitch angle at 90° and the stuck blade at 0°), given the IEC suggestion of a worst consequence fault simulation.

The DLCs considered with their respective objective and the number of simulations performed for each one are summarized in Table I. The batch of simulations was performed with the aeroelastic software FAST, over the utility size 5MW benchmark WT defined by NREL in [16]. The complete set of degrees of freedom (for an On-shore WT) was activated.

IV. RESULTS

A. Fatigue Loads Analysis

Table II presents, the LDELS variation for both FPR and APR strategies with respect to the conventional maximum power tracking strategy for the LPV controller. In this table, negative (positive) values depict loading decrease (increase). It can be seen that the effects are quite different among APC strategies. Both 90 and 80 % cases show an impaired performance for FPR strategy except for PT and IP bending moments. APR shows flatter results: it has a negligible detriment for the tower loads in the 90 and 80% cases, and it diminishes the loads in a more evenly distributed way. For both strategies, the resulting loads diminish as the power reference does.

Table III summarizes the impact of applying APC to an extended operating version of the conventional PI controller defined in [16]. For FPR strategy, PI controller exhibits similar results as the LPV, but the loading increase is even higher for the 90 and 80% cases. The improvement with respect to the baseline PI strategy for the 60 and 40% cases is a little better, resulting in a much more heterogeneous behavior of the loads. Again, the APR presents similar variations for all cases, except for the PT which shows an augmented LDEL in this case.

TABLE III
PI LDELs VARIATIONS [%].

Lifetime DELs	PI - FPR				PI - APR			
	90	80	60	40	90	80	60	40
OOP	8.4	4.0	-12.8	-24.6	1.3	-1.4	-8.1	-18.4
IP	-0.1	-1.7	-2.6	-3.3	-0.1	-0.5	-1.2	-1.8
PT	-3.7	14.9	-4.3	-18.4	-2.5	16.7	7.1	-9.0
FA	16.7	12.1	-1.8	-10.4	3.6	3.0	0.7	-4.3
SS	8.0	-10.3	-14.0	-16.1	1.1	0.3	-0.3	-1.0
HSST	38.8	22.9	-7.5	-26.6	-2.3	-8.7	-17.3	-20.8

TABLE IV
FRACTIONAL POWER REFERENCE EXTREME LOADS VARIATIONS [%].

Controller & Scenario	Ref	RS	TTC	IP	OOP	PT	SS	FA	HSST
LPV considering design situations 1 & 2 (without Parked cases)	40	-1.9	32.7	-7.8	-27.6	-35.1	-13.8	-4.3	-45.8
	60	-2.3	31.2	-6.8	-21.3	-33.7	-9.8	-4.3	-25.5
	80	-2.1	13.5	0.4	-20.1	-17.7	4.7	7.0	-14.7
	90	-0.5	6.9	2.9	-3.5	-14.6	-6.2	-1.9	-6.3
LPV considering the full load suite (with Parked situations)	40	-1.9	32.7	0.0	0.0	0.0	0.0	-0.2	-12.5
	60	-2.3	31.2	0.0	0.0	0.0	0.0	-0.2	-12.5
	80	-2.1	13.5	0.0	0.0	0.0	0.0	7.0	-12.5
	90	-0.5	6.9	0.0	0.0	0.0	0.0	-0.2	-6.3
PI considering design situations 1 & 2 (without Parked cases)	40	-5.1	43.6	-8.9	-4.1	-45.4	-12.8	-19.5	-38.4
	60	-3.5	32.1	-8.0	2.5	-49.1	-6.3	-19.5	-25.8
	80	-1.7	19.2	-3.4	2.6	-43.7	0.3	-12.8	-14.1
	90	-0.8	5.7	-2.2	-0.2	-42.9	-1.8	-6.4	-5.8
PI considering the full load suite (with Parked situations)	40	-5.1	43.6	0.0	0.0	0.0	0.0	-15.2	-12.3
	60	-3.5	32.1	0.0	0.0	0.0	0.0	-15.2	-12.3
	80	-1.7	19.2	0.0	0.0	0.0	0.0	-12.8	-12.3
	90	-0.8	5.7	0.0	0.0	0.0	0.0	-6.4	-5.8

B. Extreme Loads

The extreme loads for both LPV and PI controllers with APC in comparison with the baseline strategy are presented in Table IV and Table V for FPR and APR, respectively. They are calculated with respect to the 100% reference power of each controller. In addition to the loads considered in the previous fatigue analysis, the Rotor Speed (RS) and Tower-Tip Clearance (TTC) (i.e., the minimum distance between the tip of the blade and the tower) were incorporated to the extreme load analysis.

Each table is split into four sections: the two on top correspond to the LPV controller without and with the consideration of the parked scenarios, whereas the two on the bottom show the same results for the PI controller. From the cases without considering parked scenarios, conclusions about the performance of the controllers and how they impact extreme values can be obtained. It is important to make clear that, if these extrema are dominated by the parked cases, the obtained extreme data will turn irrelevant since they will not represent the actual extreme case of the load.

From Table IV, it can be concluded that, for the FPR strategy, the HSST extreme is reduced and there are no important increases in the extreme loads, with the exception of a 7% increment in the FA maximum for the LPV at 80%. The general trend for the rest of the power references is a decrease in most loads if the parked scenario is not considered. On the

TABLE V
ABSOLUTE POWER REFERENCE EXTREME LOADS VARIATIONS [%].

Controller & Scenario	Ref	RS	TTC	IP	OOP	PT	SS	FA	HSST
LPV considering design situations 1 & 2 (without Parked cases)	40	-1.9	17.8	-8.3	-22.0	-30.2	-14.0	-6.5	-45.7
	60	-1.7	7.9	-6.8	-22.9	-18.5	-9.1	-5.8	-25.3
	80	-1.2	7.7	0.5	-0.2	-15.0	5.0	-5.9	-13.4
	90	-0.9	2.6	2.3	-0.2	-8.8	-5.6	-0.8	-5.8
LPV considering the full load suite (with Parked situations)	40	-1.9	17.8	0.0	0.0	0.0	0.0	-0.2	-12.5
	60	-1.7	7.9	0.0	0.0	0.0	0.0	-0.2	-12.5
	80	-1.2	7.7	0.0	0.0	0.0	0.0	-0.2	-12.5
	90	-0.9	2.6	0.0	0.0	0.0	0.0	-0.2	-5.8
PI considering design situations 1 & 2 (without Parked cases)	40	-7.1	25.9	-8.9	-3.9	-45.5	-12.8	-19.2	-38.4
	60	-4.0	0.7	-8.0	-2.1	-41.0	-6.3	-5.7	-25.8
	80	-4.0	-3.0	-3.4	-4.9	-39.2	0.3	-5.5	-14.1
	90	-4.0	-0.2	-2.2	-2.4	-40.4	-1.8	4.1	-5.8
PI considering the full load suite (with Parked situations)	40	-7.1	25.9	0.0	0.0	0.0	0.0	-15.2	-12.3
	60	-4.0	0.7	0.0	0.0	0.0	0.0	-5.7	-12.3
	80	-4.0	-3.0	0.0	0.0	0.0	0.0	-5.5	-12.3
	90	-4.0	-0.2	0.0	0.0	0.0	0.0	4.1	-5.8

other hand, if they are considered, as all blade loads and the SS are dominated by the parked simulations, the decrease is limited to the FA and HSST.

Table V shows the results for the APR strategy. It can be observed that the 90% PI shows a 4.1% increase in the FA and the 80% PI a decrease of the minimum TTC of 3%. Again, the common result is that for both controllers, when considering the whole load analysis, there are almost no detrimental results. It can be seen that there are no significant differences, and that the majority of the results imply that the APC impact would be negligible or would induce a decrease in the maximum load obtained. In addition, most of the extreme loading is due to the parked cases, except for the FA and the HSST.

C. Statistical Extrapolation of Extremes

As mentioned in the previous section, DLC 1.1 consists on the extrapolation of local maxima to estimate the extreme values that have a probability of occurrence of 10 minutes within 50 years. The variation respect to each baseline case (i.e., each entry in the Tables represents the relative difference between the 50-y load obtained for each case and the one obtained for the baseline of the respective controller) for the analyzed loads are presented in Table VI and Table VII for FPR and APR strategies, respectively. As a general observation, the extrapolated extreme of the FA shows a significant increase for both APC strategies and both controllers with power references of 80 and 60%. Both OOP and PT show also an increase for some particular cases, showing a higher risk of an extreme load arising for a WT working with APC. Of course, all loads presented in these tables have a very low probability of occurrence, but the fact is that with this extrapolation there are worse extremes than for the baseline controllers.

TABLE VI
EXTRAPOLATED EXTREMES VARIATIONS WITH FPR (PU).

Controller	Pref	OOP	IP	PT	FA	SS	HSST
LPV	90	-0.2	0.0	-0.2	1.7	0.0	-0.1
	80	1.8	-0.1	-0.4	1.9	0.0	-0.4
	60	-0.3	-0.1	1.7	1.2	0.0	-0.6
	40	-0.2	-0.1	0.0	-0.2	0.0	-0.9
PI	90	-0.1	-0.1	2.2	-0.2	-0.1	0.1
	80	-0.3	-0.1	0.0	1.8	-0.1	-0.3
	60	-0.4	-0.2	0.0	0.9	-0.1	-0.5
	40	-0.3	-0.1	0.0	-0.3	-0.1	-0.8

TABLE VII
EXTRAPOLATED EXTREMES VARIATIONS WITH APR (PU).

Controller	Pref	OOP	IP	PT	FA	SS	HSST
LPV	90	-0.1	-0.1	-0.1	-0.1	0.0	-0.1
	80	-0.2	-0.1	-0.3	1.4	0.0	-0.4
	60	1.8	-0.1	-0.3	1.7	0.0	-0.9
	40	-0.2	-0.1	-0.2	-0.2	0.0	-0.9
PI	90	-0.1	0.0	2.3	-0.2	0.0	0.3
	80	-0.2	-0.1	0.1	-0.2	0.0	-0.2
	60	1.1	-0.1	0.0	1.5	-0.1	-0.6
	40	-0.2	-0.1	0.1	-0.2	0.2	-0.8

V. DISCUSSION

The load analysis carried out in this paper provides important information regarding the application of APC in WT and wind farms. Two different control schemes (LPV and PI) and two APC strategies (FPR and APR) have been assessed. For each controller-strategy combination, four levels of power reference have been considered. For comparative purposes, both controllers with a baseline control strategy have been also analyzed, totalling 18 cases studied.

Regarding fatigue loads, the main result is that using LPV-APR control, there are no negative implications whatsoever, i.e., all results lead to reductions in lifetime loads or negligible increases. The same APC strategy but with the PI controller has a similar performance, although it shows some small increases of the lifetime fatigue for the FA load at 90 and 80%, and a much more important increase in the PT at 80 and 60%. From the analysis performed, it can be said that the detriment on the PT is distributed along all wind speeds above rated. The FA increase is given at rated and below wind speeds.

Considering the FPR strategy, the results are not so good. While they present a load mitigation with both controllers for 60 and 40% power demand, the 90 and 80% deratings have detrimental implications. In the case of LPV-FPR, both tower loads exhibit an increase for 90 and 80% cases. Further, the shaft torque and the OOP raise up to 40% and 4.5% for the 90% power reference, respectively. Applying FPR to the PI controller yields similar results for the shaft torque, but deteriorate further both the tower loads and the OOP. The results of these DELs against wind speed showed that the tower loads and shaft torque increases for the LPV are located around rated. Comparable findings for the PI controller are presented in [15], where a load analysis is performed

over a 40m rotor WT, the CART3. While it is a mid-scale WT, the authors state that the CART3 WT is expected, in most situations, to represent a utility-size WT. However, two main differences have been found: first, the CART3 does not show any deterioration for the HSST, and second, the CART3 has a detriment in the edgewise moment that the simulations performed in this paper did not. In fact, the result of this work for the IP is mainly stable.

The extreme analysis shows only decrease, or no differences. Even more, most extreme loads were dominated for the parked cases, except for the FA and HSST. This is in accordance with [15], where the authors found that all extreme loads were dictated by the parked cases, but made the exception with respect to the tower loads, stating that in a utility-size WT it would not be so.

Considering these results, it can be concluded that APR offers better performance than FPR regarding fatigue loads, particularly for wind speeds close to rated. It should be noticed however that APR cannot offer reserve at wind speeds below rated. One clear solution to the fatigue load increase when applying FPR would be to distribute the reserve unevenly among WTs, such to provide the needed reserve but with some WTs performing APC and others working at 100%. This would not only avoid the detriment but would improve the fatigue loading of the WTs working with FPR at 60% or lower. Of course, this solution would only be possible depending on the desired power reserve and the available power, and could also be designed by considering the wake effect present in a wind farm.

It is important to notice that the lifetime fatigue loads obtained in this paper consider the hypothetical scenario of the WT working its entire lifetime with the same control strategy. Though unreal, this scenario provides useful qualitative knowledge of the WT performance. In the real operation, the resulting LDELs will be somewhere in-between the obtained for the different strategies applied to the WT. Further, as the achieved results show, the lifetime loads are strongly dependant not only on the strategy but also on the controller. Finally, it is noteworthy to mention that the load variations [%] for each controller listed in tables along the paper are calculated with respect to the baseline strategy applied to the same controller. For example, the load variation for LPV-APR at 60% is calculated with respect to the LPV controller with baseline strategy. Consequently, the controllers LPV vs. PI cannot be directly compared using just the data provided in the tables. In [14], comparison is carried out between both controllers with baseline strategy. It is concluded there that LPV exhibits lower fatigue and extreme loads than PI. Thus, the outperforming features of LPV with APC are even higher than tables in this paper suggest.

VI. CONCLUSIONS

From the batch of performed simulations it can be concluded that APC directly affects WT loads. Depending on the power reference, mechanical loads may vary in different ways. For the analyzed LPV and PI controllers, a WT at 90 and 80% derating shows an improvement of its blade

loads and, depending on the APC strategy, could endure a detriment of its tower loads. These results give room to WT design considerations, and operating decisions as well. One important result is that for the LPV controller with APR strategy, WT derating does not deteriorate its lifetime. Operating their WTs in APR mode, wind farms can therefore provide ancillary services to the grid and reduce WT blade loads at the same time without increasing other loads. Since, APR strategy derates WTs only above rated wind speed, WTs required to provide reserve along the complete wind speed range should be controlled with a FPR strategy, which may affect the WTs lifetime. A smart and uneven distribution of the power reference across the wind farm could avoid operating WTs in inconvenient conditions. This could be implemented with a supervisory controller to command the power reference of each WT and decide on the APC strategy to be applied, considering the wind speed, the wake effect and the fatigue and extreme loads results obtained in this work.

ACKNOWLEDGMENTS

This work was financed by UNLP (I258), and CONICET (PIP 112-202001-00331).

REFERENCES

- [1] E. Ela, V. Gevorgian *et al.*, "Active power controls from wind power: Bridging the gaps," National Renewable Energy Laboratory and University of Colorado and Electric Power Research Institute, Tech. Rep., 2014.
- [2] I. Komusanac, G. Brindley *et al.*, "Wind energy in europe," Tech. Rep., 2022.
- [3] T. Castillo, F. García *et al.*, "Panorama energético de américa latina y el caribe," OLADE, Tech. Rep., 2022.
- [4] E. Marinozzi and A. Lesce, "Informe anual 2021," CAMMESA, Tech. Rep., 2022.
- [5] F. D. Bianchi, H. De Battista, and R. J. Mantz, "Optimal gain-scheduled control of fixed-speed active stall wind turbines," *IET Renewable Power Generation*, vol. 2, pp. 228–238, apr 2008.
- [6] M. Vali, V. Petrovic *et al.*, "Model predictive active power control of waked wind farms," in *2018 Annual American Control Conference (ACC)*. IEEE, jun 2018.
- [7] H. Luo, Z. Hu *et al.*, "Coordinated active power control strategy for deloaded wind turbines to improve regulation performance in AGC," *IEEE Transactions on Power Systems*, vol. 34, no. 1, pp. 98–108, jan 2019.
- [8] X. Tang, M. Yin *et al.*, "Active power control of wind turbine generators via coordinated rotor speed and pitch angle regulation," *IEEE Transactions on Sustainable Energy*, vol. 10, no. 2, pp. 822–832, apr 2019.
- [9] S. Siniscalchi-Minna, F. D. Bianchi *et al.*, "A wind farm control strategy for power reserve maximization," *Renewable Energy*, vol. 131, pp. 37–44, feb 2019.
- [10] F. A. Inthamoussou, H. De Battista, and R. J. Mantz, "LPV-based active power control of wind turbines covering the complete wind speed range," *Renewable Energy*, vol. 99, pp. 996–1007, dec 2016.
- [11] Y. Yuan, X. Chen, and J. Tang, "Multivariable robust blade pitch control design to reject periodic loads on wind turbines," *Renewable Energy*, vol. 146, pp. 329–341, feb 2020.
- [12] H. Coral-Enriquez, J. Cortés-Romero, and S. A. Dorado-Rojas, "Rejection of varying-frequency periodic load disturbances in wind-turbines through active disturbance rejection-based control," *Renewable Energy*, vol. 141, pp. 217–235, oct 2019.
- [13] F. Pöschke, E. Gauterin *et al.*, "Load mitigation and power tracking capability for wind turbines using linear matrix inequality-based control design," *Wind Energy*, apr 2020.
- [14] B. Ibáñez, F. Inthamoussou, and H. De Battista, "Wind turbine load analysis of a full range LPV controller," *Renewable Energy*, vol. 145, pp. 2741–2753, jan 2020.

- [15] P. A. Fleming, J. Aho *et al.*, "Effects of power reserve control on wind turbine structural loading," *Wind Energy*, vol. 19, no. 3, pp. 453–469, mar 2015.
- [16] J. Jonkman, S. Butterfield *et al.*, "Definition of a 5-mw reference wind turbine for offshore system development," National Renewable Energy Laboratory (NREL), Tech. Rep., 2009. [Online]. Available: <https://www.nrel.gov/docs/fy09osti/38060.pdf>
- [17] I. E. Commission, "Iec 61400-1: Wind turbines part 1: Design requirements," International Electrotechnical Commission, Tech. Rep., 2005.
- [18] S. D. Downing and D. F. Socie, "Simple rainflow counting algorithms," *International Journal of Fatigue*, vol. 4, no. 1, pp. 31–40, Jan. 1982.
- [19] A. A. Miner, "Cumulative damage in fatigue," *ASME, Vol. 67*, 1945.
- [20] P. Veers, "Simplified fatigue damage and crack growth calculations for wind turbines," vol. -1, Jan. 1988.
- [21] G. J. Hayman, "Mlife theory manual," National Renewable Energy Laboratory (NREL), Tech. Rep., 2012.
- [22] G. Hayman, "Mextremes," National Renewable Energy Laboratory (NREL), Tech. Rep., 2015. [Online]. Available: <https://nwtc.nrel.gov/MExtremes>
- [23] P. J. Moriarty, W. E. Holley, and S. Butterfield, "Effect of turbulence variation on extreme loads prediction for wind turbines," *Journal of Solar Energy Engineering*, vol. 124, no. 4, p. 387, 2002.
- [24] M. Buhl, "Iecwind," National Renewable Energy Laboratory (NREL), Tech. Rep., 2012. [Online]. Available: <https://nwtc.nrel.gov/IECWind>



Bernabé Ibáñez was born in Junín, Buenos Aires, Argentina, in 1990. He received the B.S.E.E. degree in 2015 from La Plata National University (UNLP), Argentina. Currently he is a Professor at the School of Engineering of UNLP and a Research Assistant of the National Research Council of Argentina (CONICET). His main research interests are in control of renewable energy systems.



Fernando A. Inthamoussou was born in San Gregorio, Santa Fé, Argentina, in 1984. He received the B.S.E.E. degree in 2009 and the PhD degree in 2014, both from UNLP, Argentina. Currently he is Associate Professor at the School of Engineering of UNLP and Researcher of the CONICET. His main research interests are in nonlinear control systems, including robust, LPV, and sliding mode control.



Hernán De Battista was born in La Plata, Argentina, in 1968. He received the M.S.E. degree with highest honors in 1994 and the PhD degree in 2000, both from National University of La Plata (Argentina), where he serves now as a Full Professor. He is also Principal Researcher of CONICET and Director of the Electronics, Control and Signal Processing Research Institute (LEICI). His main research interests are in nonlinear control and its applications to renewable energies and biological systems. He received the E. Galloni award from the Argentine Academy of Exact, Physical and Natural Sciences in 2002 and the S. Gershanik award from the Buenos Aires Academy of Engineering in 2006.